Egypt. J. Chem. **Vol. 66**, No. 11 pp. 107-118 (2023)

Egyptian Journal of Chemistry

http://ejchem.journals.ekb.eg/

Gamma Radiation Effect on Normal Weight Concrete, Heavy Weight Concrete, Steel Bars, and Fiber Bars

Ahmed Abdel-Aziz[a], Mahmoud El-Fransawy[b], Mahmoud El-Desouky[b,*], and Rasha A. El-Sadany[c]

[a]*Higher Technological Institute, 6th October, Giza, Egypt.*
[b] *Faculty of Engineering-Mataria, Helwan University.*
[c] *Egyptian Atomic Energy Authority · National Center for Radiation Research and Technology.*

Abstract

This paper investigates the effects of gamma radiation for energies of 0.66, 1.17, and 1.33 MeV on the mechanical and physical properties of normal weight concrete and heavyweight concrete in addition to investigating the possibility of replacing steel bars with carbon glass fiber reinforced polymer bars. Four concrete mixtures were designed to cover the research objectives using 112 standard cubes, 108 cylinders, steel bars, and carbon glass fiber bars. These concrete mixtures were tested for their compressive strength, splitting tensile strength, and bond strength. The relationship between specimen thickness and transmission of the rays was formed by affirmation of their mean free path, half-value layer, and tenth-value layer. Also, a tensile strength test was carried out for steel and carbon glass fiber bars before and after radiation exposure. The results indicated that the use of heavyweight concrete embedded in a certain proportion of barite and ilmenite is better than normal weight concrete in radiation properties, also it's concluded that carbon glass fiber bars could be used instead of steel bars in structures exposed to gamma radiations safely.

Keywords: Radiation shielding; Linear attenuation coefficient; Gamma rays; Irradiated concrete; Normal-weight concrete; Heavyweight concrete.

1. Introduction

Concrete is a widely utilized material for providing radiation protection and acts as a shielding barrier against radiation sources such as x-ray and gamma-rays. These radiations are deemed hazardous to human health and the environment. Towards that, several studies were performed to reduce the radiation intensity to a harmless level by improving the shielding properties of both normal-weight concrete (NWC) and heavyweight concrete (HWC) [1]. Despite the wide use of the NWC in massive concrete walls for shielding purposes, still, the HWC is considered a better alternative due to; a) it has a higher resistance to radiation, b) it can absorb gamma-rays by changing or stopping their direction, and c) it is superior when the space is limited, and there is a need to reduce the thickness of the shield. The studies related to HWC differ in the aggregate types and cement ratio used in increasing the concrete density. Increasing the concrete density is vital to improving the attenuation capacity and concrete's resistance to radiation. This could be reached by a) increasing cement content and decreasing the water to binder ratio, which decreases the number of voids in concrete elements, and/or b) using additional aggregate types in the concrete mixture that could increase density, such as barite, hematite, ferrophosphorus, and magnetite [2-4]. Barite and hematite can be used as a fine and coarse aggregate and sometimes as a fine powder in a concrete mixture to increase radiological protection and improve the density and shielding of concrete [5-7]. Barite has specific gravity ranges between 4 and 4.48 at 26o C [8]. It enhances the gamma-ray mass attenuation coefficients for reactive powder concrete mixes with energy less than 0.3 MeV and greater than 8 MeV [8, 9]. Akkurt et al. [10] reported that the linear attenuation coefficient could be enhanced by 46% at photon energy 1.33MeV if the conventional aggregate was replaced by barite. Saidani et al. [11] demonstrated that the compressive strength of concrete at 28 days is increased by 17% if barite was replaced by 5% of natural aggregate in the same

*Corresponding author e-mail: mahmoud.eldesouky@hotmail.com
Receive Date: 13 August 2022, Revise Date: 10 October 2022, Accept Date: 16 October 2022
DOI: 10.21608/EJCHEM.2022.156089.6756

mixture. Additional barite (> 5% of the aggregate) could decrease the compressive strength due to the degradation of concrete's mechanical properties [11]. While Gencel et al. [12] reported that using hematite up to 50% of the total aggregate in the concrete mixture can significantly affect concrete compressive strength and density. Also, the compressive strength at 28 days was enhanced by 14.3%, while the concrete density was increased by 16.6% compared with conventional concrete when hematite was used. Besides the natural materials including barite and hematite, synthetic materials such as ferrophosphorus can also improve the concrete's ability to resist gamma-ray due to its main chemical composition of iron-nano-particles (FeNP) and its high specific gravity ranges from 5.8 to 6.3 [13]. The substitution of ferrophosphorus as fine and coarse aggregate increases the density to 42.9 KN/m3 and improves the linear attenuation coefficient by 64.6% at photon energy 1.33 MeV compared to normal concrete [14]. Another proposed approach to increase the concrete density is adding heavy elements to the concrete mixtures, such as lead, barium, or ferrite [14]. Lead is considered a suitable element that could improve the gamma attenuation properties of concrete when used as an additive powder of fine aggregate in a concrete mixture [15,16]. Rezaei and Azimkhani [15] found that the linear attenuation coefficient of concrete with 90% lead is approximately 1.58 times higher than the concrete without lead; this was based on gamma-ray emission from Cs-137 source. Lead has high significance in increasing the concrete resistance to radiation; however, due to lead's cost and its adverse effects on health since it is considered a toxic element, researchers recommended alternative eco-friendly shielding approaches by using other normal aggregates to get high-density concrete.

1.1 Research gap

In this regard, recent studies have improved the shielding properties of the concrete by using different aggregate types and cement ratios to increase the concrete density and reduce the radiation intensity to harmless levels. However, two fundamental gaps remain. Most notable is the lack of using the ilmenite as a fine aggregate in the concrete mixtures even though it has 41% titanium and 50% iron oxides that provide high comprehensive strength resistance when exposed to the radiation. Secondly, to the best of our knowledge, no study exposed the reinforced bars (steel and carbon) to radiation.

1.2 Research Significance

The present study overcomes these gaps and investigates the mechanical, physical, and radiation properties of both NWC and HWC. Furthermore, it investigates the possibility of replacing steel bars with Carbon Glass Fiber Reinforced Polymer (CGFRP) bars. In this regard, two concrete mixtures of NWC are used for both F_{cu} of 40 Mpa and 30 Mpa. In addition, two concrete mixtures of HWC with F_{cu} of 40 Mpa and 50 Mpa are embedded in a certain proportion of barite and ilmenite. These concrete mixtures are tested for their compressive strength, splitting tensile strength, and bond strength. Furthermore, the relationship between specimen thickness and transmission of the rays is formed by affirming their mean free path, half-value layer, and tenth-value layer. Finally, a tensile strength test was carried out for steel and carbon glass fiber bars before and after exposure to radiations to investigate whether carbon glass fiber bars could be used instead of steel bars in structures exposed to gamma radiations or not [16].

2 Experimental Program

This section covers the materials used in concrete and reinforcement bars. It includes the design of concrete mixtures and explains the casting and curing of the test specimens. Finally, it defines the testing methodology and the radiation shielding properties used in this study.

2.1 Materials

2.1.1 Cementitious Materials

The cementitious material used in all concrete mixtures is Ordinary Portland Cement (OPC) with (CEM I 42.5 N). It is produced by Tourah cement company in Egypt, which attains the requirements of E.S.S 4756-1/2013 [17] and E. 197-1/2011 [18]. The chemical composition of cementitious materials is presented in Table 1.

In addition, micro-silica (silica fume) produced in Egypt by SIKA company for chemical materials is used to improve strength in all the concrete mixtures. The properties of silica fume follow the ASTM C 1240 [19], and it is as follows: appearance is solid and grey powder, particle size is 0.2 µm, the surface area is 14 m2/g, density is 20 KN/m3, and PH is between 6 and 8.

Table 1 Chemical composition of cementitious materials

%	SiO_2	Al_2O_3	CaO	MgO	Fe_2O_3
OPC	19.8	5.5	63	1.18	3.39
SF	92	0.2	0.3	---	0.4
%	Na_2O	K_2O	SO_3	Loss of Ignition (LOI)	
OPC	0.46	0.16	3.01	5.2	
SF	---	---	0.1	2	

2.1.2 Aggregates

The used aggregate is a mix of coarse aggregate (i.e., dolomite - barite) and fine aggregate (i.e., sand - ilmenite). In NWC mixtures, the crushed stone (dolomite) was used as a coarse aggregate with a specific gravity of 2.7 while natural sand was used as fine aggregate with a specific gravity of 2.53. The physical properties of the natural sand are shown in

Table 2. The HWC mixtures consist of normal weight aggregate (dolomite and sand) in addition to heavy weight aggregate (barite) as a coarse aggregate and (ilmenite) as a fine aggregate, with a specific gravity of 4.48 and 4.8, respectively.

Table 2 Physical properties of fine aggregate (sand)

Property	Value	Limits *
Specific gravity (SSD)	2.53	—
Unit weight (KN/m3)	15.3	—
Fineness modulus	2.5	—
Clay and other fine materials (%)	1.5	≤ 3 %

*According to ASTM C 117 [25]

The maximum coarse aggregate size in NWC and HWC was 9.5 mm. The sieve analysis results of coarse and fine aggregates are displayed in Fig. 1, following the American Society for Testing and Materials (ASTM). The two figures show that both coarse and fine aggregates used in NWC and HWC are within the limit of sieve analysis of ASTM C 33 [20].

2.1.3 Super-Plasticizer

The Sikament-NN was used as a super-plasticizer that complies with ASTM C494 Type (F) [21] and BS 5075 Part3 [22]. The properties of Sikament -NN are shown in Table 3.

Table 3 Properties of Superplasticizer (Sikament -NN)

Base	Naphthalene Formaldehyde Sulphonate
Appearance	Brown liquid
Density (KN/m^3)	12
Chloride content	Zero
Air entrainment	Approximately zero
Compatibility	All types of Portland cement

*According to ASTM C 494 Type F [27] and BS 5075 Part 3 [28]

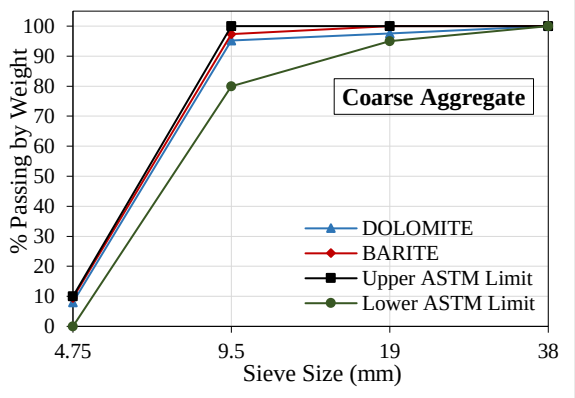

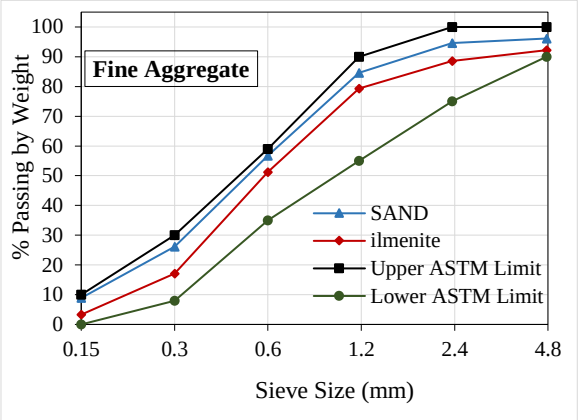

Fig. 1 Sieve analysis of coarse and fine aggregates *(according to ASTM C 33 [20])

2.1.4 Reinforcement Bars

The reinforcement bars used in this study include steel bars and Carbon Glass Fiber Reinforced Polymer (CGFRP) bars. The steel bars are high tensile steel with grade 52. Their mechanical properties are as follows: the diameter is 12 mm, the yield stress is 411 MPa, ultimate stress is 628 MPa, weight per meter is 8.88 N, density is 78 KN/m^3, and elongation is 17.7%.

The Carbon Glass Fiber Reinforced Polymer bars are formed with a density of 1.764 KN/m^3 by adding Carbon tire 330 powder to the manufactured Glass fiber and following the ASTM Vol. 09.01 [23]. The glass fiber is produced by CAMELYAF company in Turkey with a specific gravity of 2.54, a TAX of 2400 (TAX= weight in grams of 1 Km length of roving), a tensile strength of 3250 MPa, elongation of 4.5%, and diameter of 12 mm. Polyester resin used is TOPAZ 2200 NT from ICR company in addition to peroxide.

2.2 Mix Design

Four trail mixes were designed to give compressive strength of 40 MPa. The first two mixes are for NWC and designed according to ACI 211.1-91 [24] with a unit weight of 24 KN/m^3. The last two mixes are for HWC and designed according to ACI 304.3R-96 [25] with a unit weight of 38 KN/m^3. The material quantities for the concrete mixtures are listed in Table 4.

Table 4 Material quantities for the four concrete mixtures

Mixture ID	Mixture code	W/C	Concrete Ingredients (Kg/m^3)							
			Cement	Water	Coarse aggregate		Fine aggregate		Silica fume	Plasticizer
					Dolomite	Barite	Sand	ilmenite		
M-1	NWC	0.47	375	175	960	-	680	-	35	7
M-2	NWC	0.50	350	175	960	-	680	-	35	-
M-3	HWC	0.47	375	175	350	850	560	340	35	7

M-4	HWC	0.50	350	175	350	850	560	340	35	7

2.3 Casting and curing of test specimens

All the concrete mixtures in this study were mixed and cast in the laboratory of the Faculty of Engineering-Materia, Helwan University, and for each concrete mixture, fifteen standard cubes (150 mm x 150 mm x 150 mm) were cast to determine the compressive strength at 7 days, 28 days, and 365 days BEFORE radiation exposure. Moreover, ten standard cubes were cast to determine the compressive strength at 28 days and 365 AFTER radiation exposure. An additional three cubes for each mix were cast to determine the water absorption percentage at 28 days. Further, twelve standard cylinders with dimensions (150 mm diameter x 300 mm height) were cast for each concrete mixture to determine the splitting tensile strength at 28 days and 365 days. Anther twelve standard cylinders were also cast for each concrete mixture to obtain the bond strength between concrete mixtures and reinforcement bars. Among these specimens, six were tested BEFORE radiation exposure, and the other six were tested AFTER radiation exposure. For every six specimens groups, three were reinforced with steel bars, and the other three were reinforced with carbon glass fiber bars. An additional three standard cylinders were cast for each mix to determine the attenuation coefficient under gamma radiations.

Note that after casting all specimens, they were molded and immersed in a saturated water curing tank at 25□ C until reaching the age of testing. Fig. 2a shows specimens preparation for the pull-out test where the test was conducted at the age of 365 days, while Fig. 2b shows a part of standard cubes and cylinders after curing.

2.4 Testing methodology

In this section, all tests completed on fresh concrete, hardened concrete, and reinforcement bars are described. Fresh and hardened concrete tests were carried out at the laboratory of the Faculty of Engineering-Materia, Helwan University. While the tensile test for steel and fiber bars was tested at Housing and Building National Research Center (HBRC). Radiation tests were done at National Center for Radiation Research and Technology, Egyptian Atomic Energy Authority.

a) Pull-out test specimens' preparation

b) Part of standard cubes and cylinders after curing

Fig. 2 A sample of the standard cubes and cylinders used in the experimental tests

2.4.1 Determination of fresh concrete properties

The slump test is used to measure the workability and consistency of fresh concrete mixtures instantly after mixing, according to BS EN 12350-2:2009 [26].

2.4.2 Determination of hardened concrete properties

Density and compressive strength tests:

The density test is used to ascertain the bulk density of concrete. The compressive strength test is a mechanical test for measuring the maximum amount of compressive load that the concrete can bear before fracturing.

The tests were carried out on the concrete specimens (i.e., standard cubes 150 mm x 150 mm x 150 mm) according to BS EN 12390-3:2009 [27]. The specimens were submerged in water until the time of the test. The compressive strength was determined at 7 days, 28 days, and 365 days.

Water absorption:

This property is evaluated for the concrete specimens according to BS 1881-122:2011+A1:2020 [28]. It measures the amount of water maintained in the pores

using Equation 1. The W_D represents the weight of the oven-dry cube specimen, and W_S represents the weight of the saturated cube specimen.

$$WA\% = [(W_S - W_D)] / W_S \quad (1)$$

Splitting tensile strength test

It was performed according to BS EN 12390-6-2009 [29] at 28 days and 365 days using standard cylinders (150 mm diameter x 300 mm height). The splitting tensile strength of concrete (f_t) was calculated using Equation 2; where P is the maximum applied load indicated by the testing machine, d is the diameter of the specimen, and L is the length of the specimen.

$$f_t = 2\,p / \pi . d . L \quad (2)$$

Pull-out test

It was conducted to determine the bond strength between concrete and embedded steel or fiber rebars at 365 days, according to ASTM C882-99 [30]. The selected specimens were concrete cylinders (150 mm x 300 mm), where each cylinder has full-height embedded rebar with a 400 mm free end to apply the test.

2.4.3 Determination of tensile strength: steel and CGFRP bars

The tensile strength test was performed using a single-purpose testing machine according to ASTM A370 [31]. The CGFRP bars have a special setup to apply tension tests to avoid destroying the bars' tip from the grip of the machine, hence, an epoxy resin was used to assemble steel pipes with the end of fiber bars.

2.5 Radiation shielding properties

2.5.1 Measurement of gamma ray shielding properties

Radiation is a form of energy that travels in the form of electromagnetic particles through the surrounding space and can change the surrounding materials. This change depends on the radiation source, type of source, and the amount of energy generated. Attenuation is defined as a reduction in the intensity of a gamma-ray beam caused by photon absorption or deflection (scattering) from the beam [32].

The shielding tests for rays were performed using Cobalt-60 (Co-60) source of activity for about 1 µcr (microcurie). The test was carried out on different thicknesses 20 mm, 40 mm, 60 mm, 80 mm, and 100 mm, cut from the cylinder specimens.

$$\mu = (1/x) * \ln (I_0/I) \quad (3)$$

thicknesses 20 mm, 40 mm, 60 mm, 80 mm, and 100 mm, cut from the cylinder specimens.

Na I detector is used to measure the gamma activity behind the shield. It is connected to a Multi Computerized Analysis (MCA), as shown in Fig. 3a. The MCA produces peak curves of the source materials at each thickness. Photon energy was 1.333 MeV, and the radiation source is (Co-60), which is installed in a cylindrical lead shield where radiation is permitted through a small window. Each concrete specimen is placed between the gamma ray's source and the collimator, as shown in Fig. 3b. The testing time for each specimen is around 15 min.

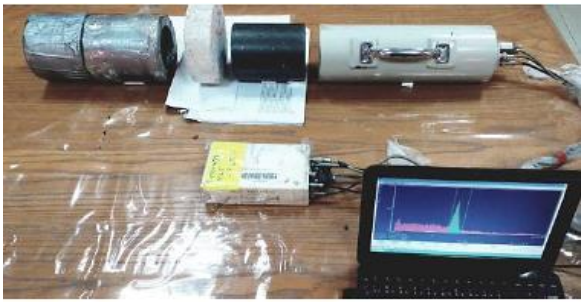

a) Attenuation coefficient experimental setup

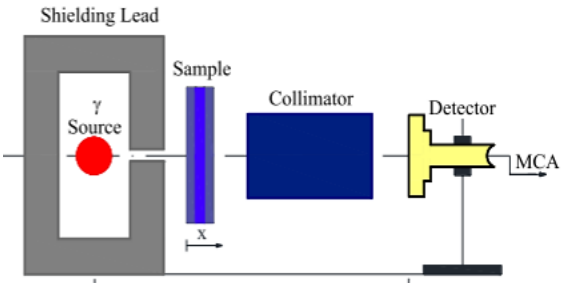

b) Narrow beam geometrical setup

Fig. 3 The attenuation coefficient measurement test [32].

2.5.2 Attenuation coefficient measurement

The shielding ability of the concrete can be measured through linear attenuation coefficient µ (cm-1) according to Beer–Lambert's law (Equation 3), which is described as the fraction of a beam of gamma rays that were absorbed or scattered per unit thickness of the absorber. The gamma-ray intensity of un-attenuated photon is defined as I_o, while the attenuated intensities through the concrete specimens with thickness x are defined as I. The average distance that gamma-ray travels in the absorber before interacting is known as the mean free path (MFP) $\bar{X}$(cm) and can be estimated using Equation 4.

$$\bar{X} = 1/\mu \quad (4)$$

The half-value layer (HVL) (Equation 5) is the thickness (mm or cm) where 50% of the incident energy has been attenuated for any given material. HVL is photon energy-dependent, where any increase in the penetrating energy of a photon stream will increase the HVL of a material.

$$HVL = ln2/\mu \quad (5)$$

The tenth value layer (TVL) (Equation 6) represents the thickness of a shield or absorber that decreases radiation levels by one-tenth of the initial level. TVL is a raw quantitative factor commonly used to represent the penetrating capability of specific radiations through a material.

$$TVL = Ln10/\mu \quad (6)$$

3 Results and Discussion

3.1 Fresh and mechanical concrete properties

It comprises the fresh concrete properties and the mechanical properties of the four concrete mixtures. It includes the results of the slump test, density, water absorption, comprehensive strength, and splitting tensile strength. The results represent the average of measurements according to the number of specimens in each test.

3.1.1 Slump, density, and water absorption

The concrete slump test results are 9 mm for M-1, M-2, M-3, and 10 mm for M-4. The density varies among the concrete mixtures where M2 has lowest density with 2300 kg/m3 and M-3 has the highest density with 3110 kg/m3. The density of the HWC (i.e., M-3 and M-4) is higher than the NWC (i.e., M-1 and M-2), as shown in Fig. 4. That, in turn, will lead to more efficiency of shielding when using the HWC. The water absorption of the M-1, M-2, M-3, and M-4 is 5.21%, 5.39%, 4.41%, and 4.47%, respectively. That indicates the high absorption of the NWC compared to the HWC.

3.1.2 Compressive strength of concrete (F_{cu})

The comprehensive strength (F_{cu}) results before and after the radiation exposure are listed in Table 5 for all the concrete mixtures. Concerning the NWC, before the radiation exposure, the M-1 mixture achieves a compressive strength (F_{cu}) of 40 MPa after 28 days, which increases to 45 MPa after 365 days. The M-2 mixture achieves compressive strength (F_{cu}) of 31 MPa after 28 days and improves to be 35 MPa after 365 days. On the other hand, after the radiation exposure, the F_{cu} of the M-1 mixture is decreased by 12.5% at 28 days and 23.33% at 365 days, as shown in Fig. 5. Similarly, the F_{cu} for the M-2 mixture diminishes constantly by 9.67% and 34.28% at 28 days and 365 days, respectively.

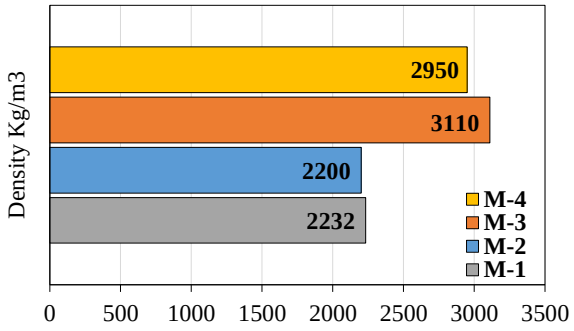

Fig. 4 Variation of density between NWC and HWC mixtures.

Table 5 Compressive strength results for all concrete mixtures

Mixture ID	Mix code	Compressive Strength (N/mm^2)				
		Before radiation (B.R)			After radiation (A.R)	
		7 days	28 days	365 days	28 days	365 days
M-1	NWC	30.5	40	45	35	34.5
M-2	NWC	22	31	35	28	23
M-3	HWC	36	50	55	50	54
M-4	HWC	30.3	40	45	40	44.5

Regarding the HWC, before the radiation exposure, the M-3 and M-4 mixtures reach the F_{cu} of 50 MPa and 40 MPa respectively, after 28 days. Though, after 365 days, F_{cu} increase for both mixtures' to be 54 MPa and 45 MPa, as shown in Fig. 6. After the radiation exposure, the F_{cu} after 28 days remains the same as before the radiation exposure. However, after 365 days, the F_{cu} is slightly decreased for M-3 and M-4 mixtures by 1.82% and 1.11%, respectively.

The results of compressive strength suggest that HWC is the ideal solution to decrease the radiation effect on structures than using NWC since the F_{cu} of NWC decreases along the structure lifetime after radiation exposure. Furthermore, the heavy concrete mixtures are slightly decreased than before radiation exposure; however, the compressive strength is generally increasing along the structure lifetime.

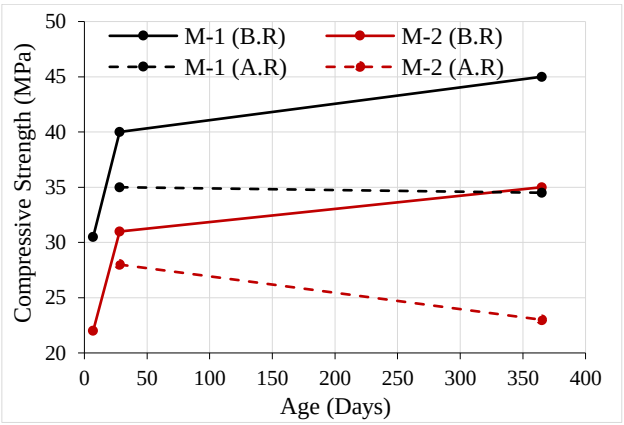

Fig. 5 Compressive strength before & after radiation (NWC).

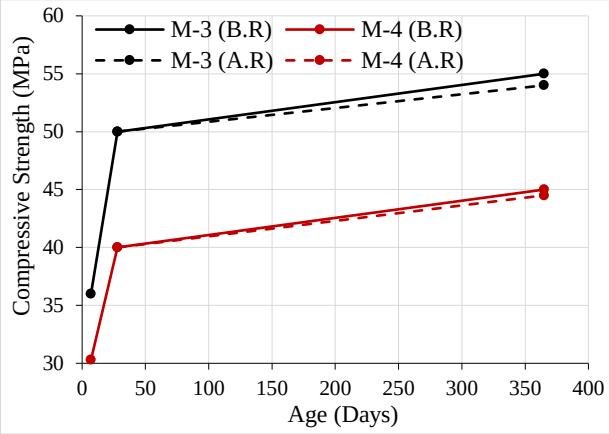

Fig. 6 Compressive strength before & after radiation (HWC).

3.1.3 *Splitting tensile strength results*

The splitting tensile strength results for the concrete mixtures before and after radiation exposure at 28 and 365 days are listed in Table 6. Ahead of the radiation exposure, the splitting tensile strength at 28 days is comparable to the NWC mixtures of M-1 and M-2 (2.07 N/mm^2 and 2.06 N/mm^2, respectively). It increases to reach 2.35 N/mm^2 and 2.33 N/mm^2 after 365 days. While after the radiation exposure by 28 and 365 days (Fig. 7), the splitting tensile strength of M-1 and M-2 decreased steeply by 18.3% and 18.9%, respectively.

Concerning the HWC before the radiation exposure, the splitting tensile strength of the M-3 mixture increases from 2.1 N/mm^2 at 28 days to 2.41 N/mm^2 at 365 days. Similarly, the M-4 mixture increases from 2.08 N/mm^2 (28 days) to 2.39 N/mm^2 (365 days). In contrast, the splitting tensile strength after the radiation exposure decreases slightly at 28 days by 2.85% and 3.37% for both M-3 and M-4, respectively. In addition, the splitting tensile strength reduces marginally at 365 days by 3% and 3.35% for both mixtures respectively.

Table 6 Splitting tensile strength of concrete cylinders

Mix	Mix code	Splitting tensile strength (N/mm^2)			
		Before radiation (B.R.)		After radiation (A.R.)	
		28 days	365 days	28 days	365 days
M-1	NWC	2.07	2.35	1.69	1.92
M-2	NWC	2.06	2.33	1.67	1.89
M-3	HWC	2.1	2.41	2.04	2.34
M-4	HWC	2.08	2.39	2.01	2.31

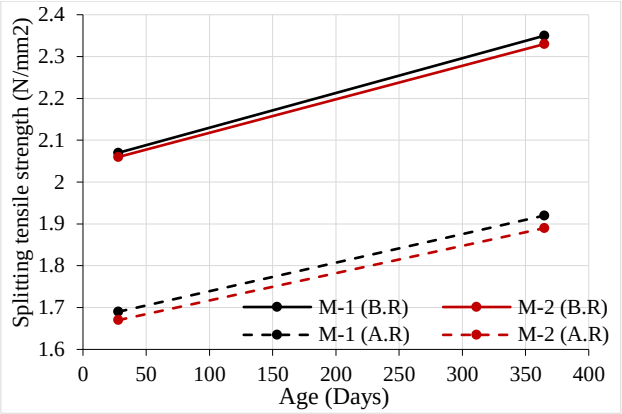

Fig. 7 Splitting tensile strength before and after radiation (NWC).

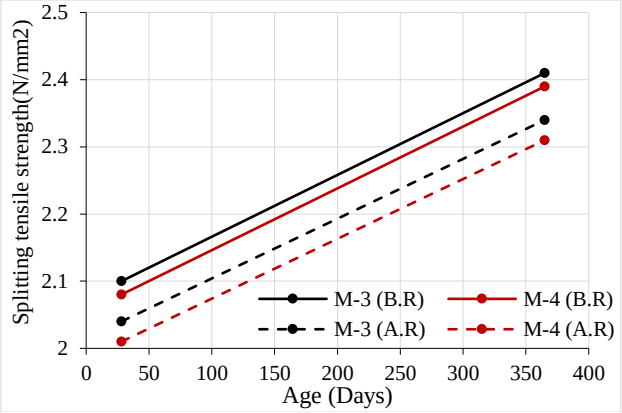

Fig. 8 Splitting tensile strength before and after radiation (HWC).

The splitting tensile strength results indicate that any decrease in its value after radiation exposure will not exceed 19% for NWC (For compressive strength between 30 to 40 MPa). While, for HWC (With compressive strength between 40 to 50 MPa), any reduction in the splitting tensile strength after radiation exposure will not surpass 3.4%; thus, the HWC is still superior to NWC.

3.1.4 *Pull-out test results*

The pull-out test results for concrete cylinders (before and after the radiation exposure) after 365 days for all concrete mixtures are listed in Table 7 (also plotted in Fig. 9) before the radiation exposure and after 365 days. The results imply that the radiation significantly impacts the bond strength for both steel and CGFRP bars in the NWC and HWC.

In the NWC, the bond strength of the M-1 mixture (F_{cu}= 40 MPa) decreases after the radiation exposure by 35.11% and 33.61% for steel and CGFRP bars, respectively. At the same time, it drops for the M-2 mixture (F_{cu}= 30 MPa) by 36.84% for steel bars and 34.13% for CGFRP bars.

Concerning the HWC, the bond strength decreases for the M-3 mixture (F_{cu}: 50 MPa) after radiation exposure by 17.85% and 29.74% for steel and CGFRP bars.

Besides, the bond strength diminishes for the M-4 mixture (F_{cu}: 40 MPa) by 17.82% for steel bars and 29.93% for CGFRP bars.

The results indicate that the NWC (i.e., M-1) and HWC (i.e., M-4) that have the same compressive strength (F_{cu}= 40 MPa), have a significant reduction in their bond strength after the radiation exposure when using the CGFRP (35% reduction) more than the steel bars (18% reduction).

In addition, after the radiation exposure, the decrement rate of bond strength when using the steel bars in NWC (M-1, F_{cu}: 40 MPa) could reach 50% less than the decrement rate of bond strength when using the steel bars in HWC (M-4, F_{cu}= 40 MPa).

By comparing the usage of steel and CGFRP bars in the reinforcement of the HWC mixtures (M-3 and M-4), it was found that using the CGFRP bars will reduce the bond strength by about 19% before radiation and 30% after radiation exposure. While using the CGFRP in NWC mixtures (M-1 and M-2) will reduce the bond strength by 20% before and 17% after the radiation exposure.

The results reveal that the decrement rate of bond strength after radiation exposure for HWC is lower than for NWC. Moreover, steel bars have higher resistance toward the bond strength than CGFRP before and after the radiation exposure in both NWC and HWC.

Table 7 Bond strength for steel and Carbon Glass Fiber Reinforced Polymer (CGFRP) bars

Mixture ID	Mix code	Fcu (N/mm^2)	*Bond strength for steel bars (MPa)		*Bond st (CGFR
			Before radiation	After radiation	Before radiation
M-1	NWC	40	7.49	4.86	6.04
M-2	NWC	30	7.41	4.68	5.89
M-3	HWC	50	7.56	6.21	6.12
M-4	HWC	40	7.52	6.18	6.08

* Bar diameter is 12 mm, and the embedded length is 300 mm for both steel bars and CGFRP bars.

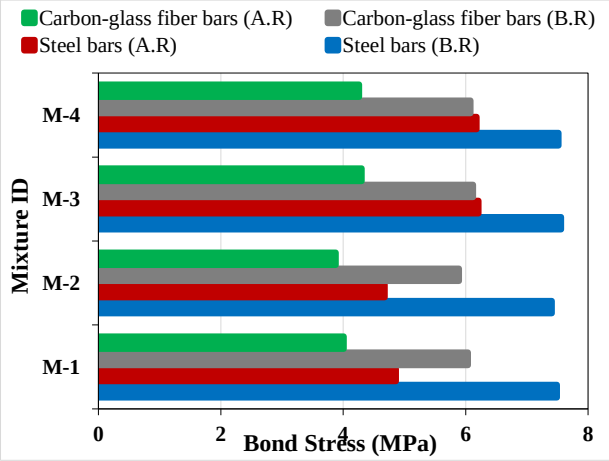

Fig. 9 Pull-out test results before and after radiation exposure for 365 days

3.2 Radiation attenuation coefficient measurement

3.2.1 Experimental measurement

The linear attenuation coefficients of NWC and HWC are presented in Table 8 for each gamma-ray energy (0.66, 1.17 and 1.33 MeV), using Cobalt-60 and Cesium sources. Besides, the difference in intensity with thickness for different photon energy is shown in Table 9. The mean free path (MFP), half-value layer (HVL), and tenth-value layer (TVL), which are the most used transmission thickness of gamma-rays in shield design, are listed in Table 10 and Table 11.

Table 8 Linear attenuation coefficient for NWC and HWC at different thicknesses

E (MeV)	μ (cm^{-1}) for NWC				
	2 cm	4 cm	6 cm	8 cm	10 cm
0.66	0.148	0.135	0.127	0.123	0.119
1.17	0.136	0.129	0.123	0.121	0.114
1.33	0.134	0.125	0.122	0.118	0.113
Average	0.139	0.130	0.124	0.121	0.115
E (MeV)	μ (cm^{-1}) for HWC				
	2 cm	4 cm	6 cm	8 cm	10 cm
0.66	0.173	0.150	0.143	0.132	0.129
1.17	0.154	0.137	0.135	0.128	0.121
1.33	0.149	0.135	0.132	0.125	0.120
Average	0.159	0.141	0.137	0.128	0.123

Table 9 Variation of intensity with thickness for different photon energy (count)

Type	E (MeV)	0 cm	2 cm	4 cm	6 cm	8 cm	10 cm
NWC	0.66	54354	40447	31725	25355	20289	16476
	1.17	120120	91589	71581	57273	45661	38230
	1.33	106946	81782	64772	51430	41647	34513
HWC	0.66	53676	37994	29403	22774	18744	14844
	1.17	117229	86095	67643	52189	42071	34928
	1.33	105552	78288	61465	47936	38797	31785

4.3
4.26

Table 10 Mean free path (cm) for NWC and HWC at different thicknesses

Type	E (MeV)	2 cm	4 cm	6 cm	8 cm	10 cm
NWC	0.66	6.768	7.429	7.868	8.118	8.378
	1.17	7.375	7.727	8.101	8.271	8.735
	1.33	7.455	7.977	8.196	8.483	8.842
HWC	0.66	5.788	6.646	6.999	7.604	7.780
	1.17	6.479	7.274	7.414	7.807	8.259
	1.33	6.693	7.397	7.601	7.993	8.332

Table 11 Half and tenth value layer (cm) for NWC and HWC at different thicknesses

Type	E (MeV)	HVL (cm)				
		2 cm	4 cm	6 cm	8 cm	10 cm
NWC	0.66	4.691	5.149	5.454	5.627	5.807
	1.17	5.112	5.356	5.615	5.733	6.054
	1.33	5.167	5.529	5.681	5.880	6.129
HWC	0.66	4.012	4.607	4.851	5.271	5.393
	1.17	4.491	5.042	5.139	5.411	5.725
	1.33	4.639	5.127	5.269	5.540	5.775
Type	E (MeV)	TVL (cm)				
		2 cm	4 cm	6 cm	8 cm	10 cm

NWC	0.66	15.583	17.106	18.117	18.693	19.291
	1.17	16.982	17.792	18.653	19.045	20.112
	1.33	17.166	18.367	18.871	19.532	20.359
HWC	0.66	13.327	15.303	16.115	17.509	17.914
	1.17	14.919	16.749	17.072	17.975	19.016
	1.33	15.412	17.033	17.503	18.405	19.185

Fig. 10 and Fig. 11 illustrate the variations of linear attenuation coefficient (μ) at different thicknesses for NWC and HWC.

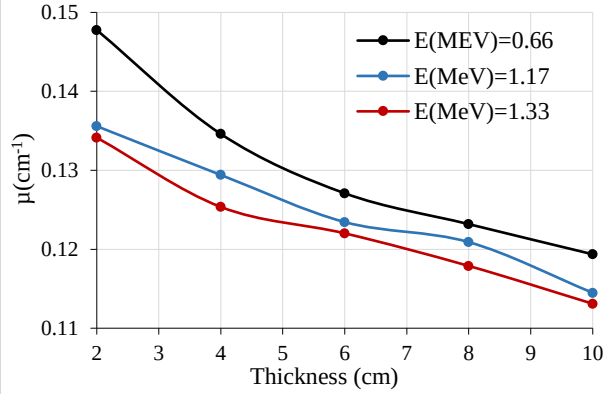

Fig. 10. Linear attenuation coefficient (μ) at different thicknesses for NWC.

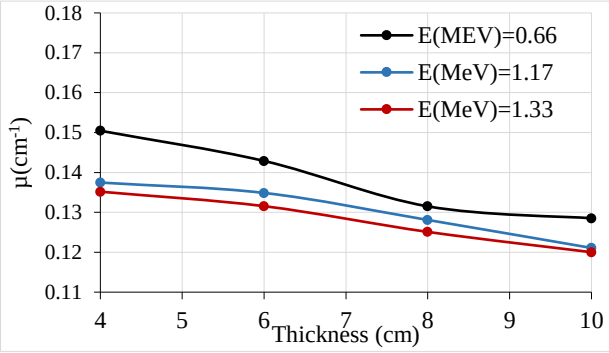

Fig. 11. Linear attenuation coefficient (μ) at different thicknesses for HWC.

It can be concluded that increasing concrete density and increment of gamma-ray energy (E) will reduce the linear attenuation coefficient at the same thickness. Consequently, the values of the MFP, HVL, and TVL will be decreased. In addition, the results demonstrate that HWC is denser than NWC, which will improve (μ) and shielding properties.

3.2.2 XCOM simulation for attenuation coefficient verification

The experimental results were verified using XCOM simulation for both normal weight concrete (N.W.C) and heavyweight concrete (H.W.C), and it showed that the results are very close in values to the experimental values as shown in figures: 12, 13, 14, and 15.

Edge	(required) Photon Energy	Scattering		Photoelectric Absorption	Pair Production		Total Attenuation	
		Coherent	Incoherent		In Nuclear Field	In Electron Field	With Coherent Scattering	Without Coherent Scattering
	MeV	cm²/g	cm²/g	cm²/g	cm²/g	cm²/g	cm²/g	cm²/g
	8.000E-01	1.958E-04	7.112E-02	5.724E-05	0.000E+00	0.000E+00	7.138E-02	7.118E-02
	1.000E+00	1.254E-04	6.397E-02	3.559E-05	0.000E+00	0.000E+00	6.413E-02	6.401E-02
	1.022E+00	1.201E-04	6.330E-02	3.364E-05	0.000E+00	0.000E+00	6.345E-02	6.333E-02
	1.170E+00	9.166E-05	5.918E-02	2.550E-05	9.487E-06	0.000E+00	5.930E-02	5.921E-02
	1.250E+00	8.030E-05	5.721E-02	2.278E-05	2.833E-05	0.000E+00	5.734E-02	5.726E-02
	1.330E+00	7.093E-05	5.540E-02	2.044E-05	5.802E-05	0.000E+00	5.555E-02	5.548E-02
	1.500E+00	5.577E-05	5.200E-02	1.647E-05	1.533E-04	0.000E+00	5.222E-02	5.217E-02
	2.000E+00	3.138E-05	4.438E-02	1.023E-05	6.046E-04	0.000E+00	4.503E-02	4.500E-02
	2.044E+00	3.005E-05	4.383E-02	9.888E-06	6.515E-04	0.000E+00	4.452E-02	4.449E-02
	3.000E+00	1.395E-05	3.491E-02	5.616E-06	1.714E-03	1.222E-05	3.666E-02	3.665E-02
	4.000E+00	7.849E-06	2.913E-02	3.809E-06	2.770E-03	4.988E-05	3.196E-02	3.195E-02
	5.000E+00	5.023E-06	2.515E-02	2.867E-06	3.708E-03	9.938E-05	2.897E-02	2.896E-02
	6.000E+00	3.488E-06	2.223E-02	2.292E-06	4.549E-03	1.526E-04	2.694E-02	2.694E-02

Fig. 12. XCOM results for NWC for different energies

Edge	(required) Photon Energy	Scattering		Photoelectric Absorption	Pair Production		Total Attenuation	
		Coherent	Incoherent		In Nuclear Field	In Electron Field	With Coherent Scattering	Without Coherent Scattering
	MeV	cm²/g	cm²/g	cm²/g	cm²/g	cm²/g	cm²/g	cm²/g
	8.000E-01	7.272E-04	6.749E-02	1.942E-03	0.000E+00	0.000E+00	7.016E-02	6.943E-02
	1.000E+00	4.677E-04	6.073E-02	1.213E-03	0.000E+00	0.000E+00	6.241E-02	6.195E-02
	1.022E+00	4.480E-04	6.008E-02	1.160E-03	0.000E+00	0.000E+00	6.169E-02	6.125E-02
	1.170E+00	3.426E-04	5.618E-02	8.880E-04	2.537E-05	0.000E+00	5.744E-02	5.709E-02
	1.250E+00	3.004E-04	5.433E-02	7.828E-04	7.223E-05	0.000E+00	5.549E-02	5.518E-02
	1.330E+00	2.655E-04	5.262E-02	6.973E-04	1.421E-04	0.000E+00	5.372E-02	5.346E-02
	1.500E+00	2.090E-04	4.938E-02	5.603E-04	3.515E-04	0.000E+00	5.050E-02	5.029E-02
	2.000E+00	1.178E-04	4.216E-02	3.408E-04	1.246E-03	0.000E+00	4.386E-02	4.375E-02
	2.044E+00	1.128E-04	4.163E-02	3.288E-04	1.335E-03	0.000E+00	4.341E-02	4.330E-02
	3.000E+00	5.243E-05	3.317E-02	1.807E-04	3.270E-03	1.161E-05	3.669E-02	3.663E-02
	4.000E+00	2.950E-05	2.767E-02	1.196E-04	5.107E-03	4.737E-05	3.298E-02	3.295E-02
	5.000E+00	1.889E-05	2.390E-02	8.837E-05	6.712E-03	9.436E-05	3.081E-02	3.079E-02
	6.000E+00	1.312E-05	2.112E-02	6.971E-05	8.121E-03	1.449E-04	2.947E-02	2.946E-02

Fig. 13. XCOM results for HWC for different energies

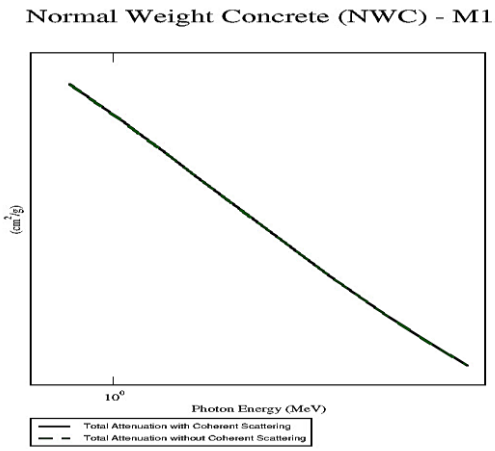

Fig. 14. XCOM graph for NWC for different energies and total attenuation

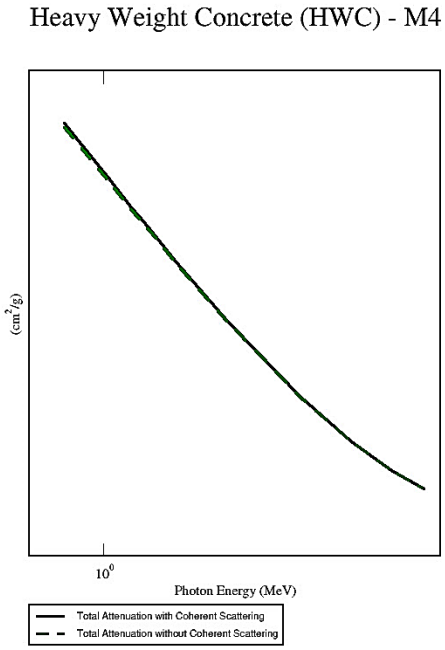

Fig. 15. XCOM graph for HWC for different energies and total attenuation

3.3 Mechanical results of reinforcement bars

The tensile test results are listed in Table 12 and plotted in Fig. 16. The results show a significant increase in the ultimate strength of steel and CGFRP bars by 32.48% and 29.50%, respectively. Also, the ductility decreases by 15.6% and 12.5% for both steel and CGFRP bars. Moreover, there is an increase in proof strength (0.2% offset of yield strength) for steel bars about 34.80%. These changes in tensile strength due to radiation exposure are called vacancies and interstitials. A vacancy is a space left behind by a displaced atom. An interstitial is an atom forced into a position that it would not naturally assume between other atoms. Therefore, atoms are knocked out of their lattice positions, leading to defects and dislocations [33].

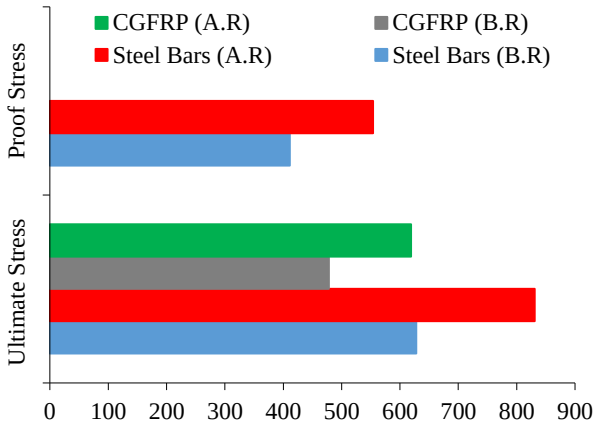

Fig. 16 Tensile strength (MPa) for steel and CGFRP bars

Table 12 Tensile strength for steel bars and CGFRP bars

	Specimen (Bar)	Ultimate Strength (MPa)	Proof Strength (MPa)	Elongation (%)
Before Radiation	Steel	628	411	17.3
	CGFRP	478	-	4.8
After Radiation	Steel	831	554	14.6
	CGFRP	619	-	4.2

4 Conclusion

This study aims at improving the mechanical properties of reinforced heavyweight concrete (HWC) structures for radiation shielding. Behind laboratory tests made on fresh and hardened concrete, the conclusion can be defined as follows:

- Heavyweight concrete is an ideal solution for decreasing the radiation impact on structures than normal-weight concrete. The high density of the heavyweight concrete improves the shielding properties, especially when using barite as coarse aggregate replacing 20% of fine aggregate with ilmenite.
- The compressive strength of standard heavyweight cubes is kept constant after exposure to radiation for 28-days. Otherwise, the compressive strength is slightly decreased for F_{cu}=40 MPa and 50 MPa by 1.82% and 1.11%, respectively, after 365 days from radiation exposure.
- The compressive strength of normal-weight concrete with F_{cu} =40 Mpa is significantly decreased after radiation exposure by 12.5% and 23.33% at 28 and 365 days respectively. While for F_{cu}=30 MPa the compressive strength decreased by 9.67% and 34.28 % at 28 and 365- days respectively.
- The decrease of splitting tensile strength after radiation exposure will not be more than 19% for normal-weight concrete, which has a value of

compressive strength between 30 to 40 MPa. Otherwise, for heavyweight concrete, whose compressive strength value is between 40 to 50 MPa, the tensile strength will not decrease more than 3.4% after radiation exposure.

- Bond strength decreased for heavy and normal-weight concrete, reinforced with steel bars for the same Fc_u by approximately 18% and 35%, respectively, after radiation exposure by 365 days. But suppose carbon-glass fiber bars (CGFRP) were used to reinforce heavyweight and normal-weight concrete. In that case, the bond strength will decrease for the same F_{cu} by approximately 30% and 34% after 365 days from the radiation exposure.
- Using carbon glass fiber reinforced polymer bars in heavyweight concrete will decrease the bond strength by 19% before radiation exposure and by 31% after exposure to radiation by 365 days than using steel bars. While using CGFRP in normal-weight concrete will decrease the bond strength by 19% before radiation exposure and 17.5% after radiation exposure by 365 days.
- Increasing concrete density and increment of gamma-ray energy (E) will reduce the linear attenuation coefficient (μ) for the same thickness. Thus, the Mean free path (MFP), half-value layer (HVL), and tenth-value layer (TVL), which are the most used transmission thickness of gamma-rays in shield design, will increase. The linear attenuation coefficient for heavyweight concrete was enhanced by 36.8% when compared with normal-weight concrete.

5 Conflicts of interest

The authors declare that they have no conflict of interest.

6 Acknowledgments

The authors would express gratitude to the lab staff members of Materia and the National Center for Radiation Research and Technology to provide us with the correct equipment needed to fulfill this research.

7 References

[1] Oluwaseun Azeez M, Ahmad S, Al-Dulaijan SU, Maslehuddin M, Abbas Naqvi A. Radiation shielding performance of heavy-weight concrete mixtures. Construction and Building Materials. 2019;224:284-91.

[2] Almeida Junior TA, Nogueira MS, Vivolo V, Potiens MPA, Campos LL. Mass attenuation coefficients of X-rays in different barite concrete used in radiation protection as shielding against ionizing radiation. Radiation Physics and Chemistry. 2017;140:349-54.

[3] Sadrmomtazi A, Lotfi-Omran O, Nikbin IM. Influence of cement content and maximum aggregate size on the fracture parameters of magnetite concrete using WFM, SEM and BEM. Theoretical and Applied Fracture Mechanics. 2020;107.

[4] Azreen NM, Rashid RSM, Mugahed Amran YH, Voo YL, Haniza M, Hairie M, et al. Simulation of ultra-high-performance concrete mixed with hematite and barite aggregates using Monte Carlo for dry cask storage. Construction and Building Materials. 2020;263.

[5] Şensoy AT, Gökçe HS. Simulation and optimization of gamma-ray linear attenuation coefficients of barite concrete shields. Construction and Building Materials. 2020;253.

[6] González-Ortega MA, Cavalaro SHP, Aguado A. Influence of barite aggregate friability on mixing process and mechanical properties of concrete. Construction and Building Materials. 2015;74:169-75.

[7] Gökçe HS, Yalçınkaya Ç, Tuyan M. Optimization of reactive powder concrete by means of barite aggregate for both neutrons and gamma rays. Construction and Building Materials. 2018;189:470-7.

[8] Mostofinejad D, Reisi M, Shirani A. Mix design effective parameters on γ-ray attenuation coefficient and strength of normal and heavyweight concrete. Construction and Building Materials. 2012;28(1):224-9.

[9] Liu H-l, Shi JJ, Qu H, Ding DJC, Materials B. An investigation on physical, mechanical, leaching and radiation shielding behaviors of barite concrete containing recycled cathode ray tube funnel glass aggregate. 2019.

[10] Akkurt I, Akyildirim H, Mavi B, Kilincarslan S, Basyigit C. Gamma-ray shielding properties of concrete including barite at different energies. Progress in Nuclear Energy. 2010;52(7):620-3.

[11] Saidani K, Ajam L, Ben Ouezdou M. Barite powder as sand substitution in concrete: Effect on some mechanical properties. Construction and Building Materials. 2015;95:287-95.

[12] Gencel O, Bozkurt A, Kam E, Korkut T. Determination and calculation of gamma and neutron shielding characteristics of concretes containing different hematite proportions. Annals of Nuclear Energy. 2011;38(12):2719-23.

[13] C637-20 A. Standard Specification for Aggregates for Radiation-Shielding Concrete. ASTM International, West Conshohocken, PA. 2020.

[14] Julphunthong P, Joyklad P. Investigation of Gamma Ray Shielding and Compressive Strength of Concrete Containing Barite and Ferrophosphorous. Key Engineering Materials. 2018;775:618-23.

[15] Rezaei-Ochbelagh D, Azimkhani S. Investigation of gamma-ray shielding properties of concrete containing different percentages of lead. Appl Radiat Isot. 2012;70(10):2282-6.

[16] Kurtulus R, Kavas T, Akkurt I, Gunoglu K. An experimental study and WinXCom calculations on X-ray photon characteristics of Bi2O3- and Sb2O3-

added waste soda-lime-silica glass. Ceramics International. 2020;46(13):21120-7.
[17] 4756-1 ESS. Egyptian organization for standard and quality, chemical, cement (part 1), composition and specifications. 2013.
[18] 197-1 EN. European standard, Cement - Part 1: Composition, specifications, and conformity criteria for common cement. 2011.
[19] C1240-20 A. Standard Specification for Silica Fume Used in Cementitious Mixtures, ASTM International, West Conshohocken, PA. 2020.
[20] C33M-18 AC. Standard Specification for Concrete Aggregates, ASTM International, West Conshohocken, PA. 2018.
[21] C494M-19 AC. Standard Specification for Chemical Admixtures for Concrete, ASTM International, West Conshohocken, PA. 2019.
[22] 3 BP. Concrete Admixtures - Part 3: Super plasticizing Admixtures, British standard. 1985.
[23] ASTM Book of Standards Volume 09.01: Rubber NaS-GTMCB. 2019.
[24] 211.1-91 A. American concrete institute, Standard Practice for Selecting Proportions for Normal, Heavyweight, and Mass Concrete.
[25] 304.3R-96 A. American concrete institute, Heavyweight Concrete: Measuring, Mixing, Transporting, and Placing.
[26] 12350-2 BE. British standard, Testing fresh concrete. Slump-test. 2009.
[27] 12390-3 BE. British standard, Testing hardened concrete. Compressive strength of test specimens. 2009.
[28] 1881-122:2011+A1 B. British standard, Testing concrete method for determination of water absorption. 2020.
[29] 12390-6 BE. British standard, Testing Hardened Concrete Part 6 - Tensile Splitting Strength of Test Specimens. 2009.
[30] C882M-20 AC. Standard Test Method for Bond Strength of Epoxy-Resin Systems Used with Concrete by Slant Shear, ASTM International, West Conshohocken, PA. 2020.
[31] A370-20 A. Standard Test Methods, and Definitions for Mechanical Testing of Steel Products, ASTM International, West Conshohocken, PA. 2020.
[32] Al-Tersawy SH, El-Sadany RA, Sallam HEM. Long-term behavior of normal weight concrete containing hybrid nanoparticles subjected to gamma radiation. Archives of Civil and Mechanical Engineering. 2021;21(1).
[33] Vértesy G, Gasparics A, Uytdenhouwen I, Szenthe I, Gillemot F, Chaouadi R. Nondestructive Investigation of Neutron Irradiation Generated Structural Changes of Reactor Steel Material by Magnetic Hysteresis Method. Metals. 2020;10(5).